Secondary structure of the MutT enzyme as determined by NMR

ARTICLE *in* BIOCHEMISTRY · JANUARY 1994

Impact Factor: 3.02 · DOI: 10.1021/bi00211a018 · Source: PubMed

4 AUTHORS, INCLUDING:

David Joseph Weber
University of Maryland, Baltimore
126 PUBLICATIONS **3,843** CITATIONS

Secondary Structure of the MutT Enzyme As Determined by NMR†

David J. Weber,‡,§ Chitrananda Abeygunawardana,‡ Maurice J. Bessman‖ Albert S. Mildvan*,‡

Department of Biological Chemistry, The Johns Hopkins School of Medicine, 725 North Wolfe Street, Baltimore, Maryland 21205, and Department of Biology, The Johns Hopkins University, Charles and 34th Streets, Baltimore, Maryland 21218

Received July 15, 1993; Revised Manuscript Received September 17, 1993®

ABSTRACT: The MutT enzyme (129 amino acids) catalyzes the hydrolysis of nucleoside triphosphates (NTP) to nucleotides (NMP) and pyrophosphate by nucleophilic substitution at the rarely attacked β-phosphorus of NTP [Weber, D. J., Bhatnagar, S. K., Bullions, L. L., Bessman, M. J., & Mildvan, A. S. (1992) *J. Biol. Chem. 267*, 16939–16942]. Backbone NMR assignments for the Hα, ^{13}Cα, HN, ^{15}N, and carbonyl ^{13}C′ resonances, based on heteronuclear methods have been reported for MutT [Abeygunawardana, C., Weber, D. J., Frick, D. N. Bessman, M. J., & Mildvan, A. S. (1993) *Biochemistry* (preceding paper in this issue)]. Here, we report the secondary structure of MutT in solution on the basis of these assignments, NOE data derived from 2D and 3D homonuclear and heteronuclear NMR spectra, and amide NH exchange data. Consistent with near neighbor NOEs, Hα and Cα chemical shifts, and amide exchange rates, MutT contains two α-helices spanning residues 47–59 (helix 1) and residues 119–128 (helix 2), respectively. The helical content predicted from NMR (17.8 ± 1.0%) is consistent with that predicted by circular dichroism spectroscopy (20.9 ± 5.4%). A mixed parallel and antiparallel β-sheet with five β-strands (A–E) consists of residues A, 3–13; B, 18–24; C, 70–74; D, 79–87; and E, 102–106. The antiparallel (a) or parallel (p) alignment of strands in the β-sheet, based on 34 assigned long-range NOE peaks and 22 slowly exchanging amide NH protons, is C(a)D(p)A(a)B(a) E where strands C and D are connected by a type I tight turn, and strands A and B are connected by a nonclassical turn. Four loops (I, 24–46; II, 59–70; III, 88–101; and IV, 107–118) adopt an irregular, but well-defined structure with changes in direction via nonclassical turns occurring between residues 66–70, 88–90, and 113–115. All nine proline residues of MutT are *trans*, based on NOEs to preceding residues. Regions of flexibility, as judged by the absence of ^{1}H–^{15}N correlations in HSQC spectra and the absence of NOEs, are found at positions 25–31, 43, 112, and 118. Changes in chemical shifts and relaxation rates of ^{15}N and NH resonances occur in loop I in response to the binding of the activator Mg^{2+} and the substrate analogs Mg^{2+}-AMPCPP and Mn^{2+}-AMPCPP. Loop I also shows sequence identities with related enzymes from other bacteria suggesting this to be a portion of the active site.

The MutT enzyme from *Escherichia coli* is a small protein (129 residues) which, in the presence of divalent cations, catalyzes the unusual hydrolysis of nucleoside and deoxynucleoside triphosphates (NTP) to yield nucleotides and pyrophosphate (Bhatnagar *et al.*, 1991), by nucleophilic substitution at the rarely attacked β-phosphorus of NTP (Weber *et al.*, 1992a). Deficiencies in this enzyme result in a large increase in AT → CG mutations in *E. coli* (Treffers *et al.*, 1954; Yanofsky *et al.*, 1966; Cox, 1973). A related enzyme activity has been reported in human cells (Mo *et al.*, 1992) and may therefore be widely distributed in nature. Hence the MutT enzyme is of interest, from both a mechanistic and biological point of view.

At present, no structures have been reported of the MutT enzyme or of any protein homologous with MutT. Moreover, among functionally related enzymes of this class, the low sequence homologies (Bullions, 1993) preclude prediction of the overall secondary structure (Rost *et al.*, 1993). The preceding paper used heteronuclear NMR methods to sequence specifically assign the backbone Hα, Cα, NH, ^{15}N, and carbonyl ^{13}C′ resonances of MutT (Abeygunawardana *et al.*, 1993b). On the basis of these assignments, the present paper analyzes near neighbor and remote interproton NOEs to obtain the solution secondary structure of this enzyme. Consistent with the stability of MutT, its secondary structure is similar to that of other highly stable proteins. Abstracts of this work have been published (Abeygunawardana, *et al.*, 1993a; Weber *et al.*, 1993a,b).

MATERIALS AND METHODS

Unlabeled and uniformly ^{15}N-labeled MutT were obtained as previously described (Abeygunawardana *et al.*, 1993b). Uniformly (99%) deuterated Tris (d_{11})[1] and [^{15}N]NH_4Cl were purchased from Cambridge laboratories. Enzyme preparations were assayed before and after each NMR experiment

† This work supported by grants from the National Institutes of Health to A.S.M. (DK28616) and to M.J.B. (GM18649).

* To whom correspondence should be addressed.

‡ The Johns Hopkins School of Medicine.

§ Present address: Department of Biological Chemistry, University of Maryland School of Medicine, 108 N. Greene Street, Baltimore, MD 21201.

‖ The Johns Hopkins University.

® Abstract published in *Advance ACS Abstracts*, November 15, 1993.

[1] Abbreviations: Tris, tris(hydroxymethyl)aminomethane hydrochloride; CD, circular dichroism; NOESY, nuclear Overhauser effect spectroscopy; ROESY, rotating frame Overhauser effect spectroscopy; HMQC, heteronuclear multiple-quantum coherence; HSQC, heteronuclear single-quantum coherence; TPPI, time-proportional phase incrementation; NMR, nuclear magnetic resonance; NN or NN (i,i+1), HN_i to HN_{i+1} NOE cross peak; NN (i,i+2), HN_i to HN_{i+2} NOE cross peak; αN or αN(i,i+1), Hα to HN_{i+1} NOE cross peak; αN(i,i+2), Hα to HN_{i+2} NOE cross peak; αN(i,i+3); Hα to HN_{i+3} NOE cross peak; αN(i,i+4), Hα to HN_{i+4} NOE cross peak; TSP, 3-(trimethyl silyl)propionate-*2,2,3,3-d*$_4$.

0006-2960/93/0432-13081$04.00/0

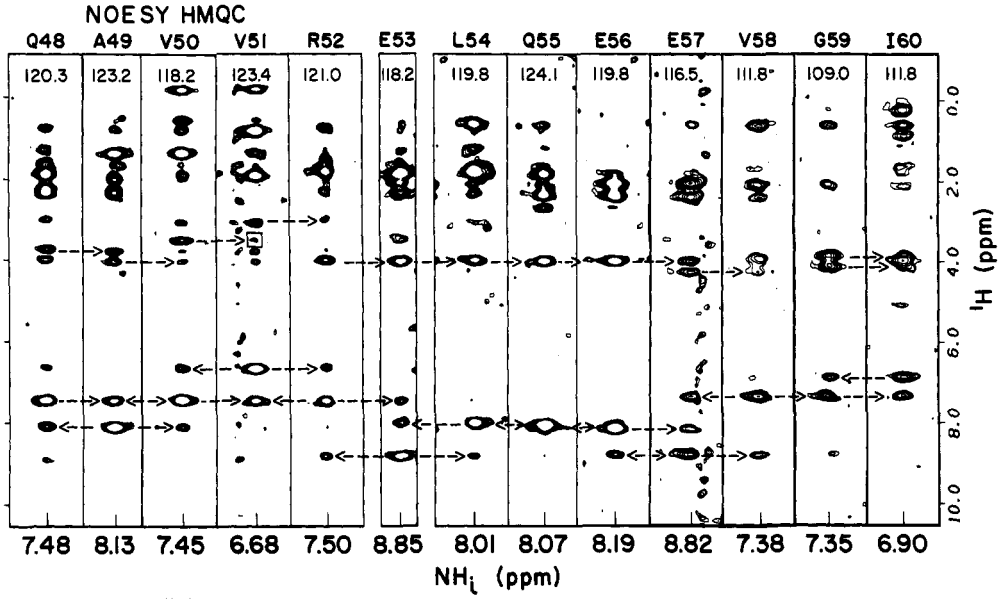

FIGURE 1: Strips extracted from ^{15}N planes of a 3D NOESY-HMQC spectrum to illustrate NOE peaks involved in helix 1 (residues 48–60). The spectrum was acquired at 32 °C with a 200-ms mixing time and processed with the NMR processing software Felix (Hare Inc.) utilizing a 90°-shifted sine bell filtering in t_3. In each strip the ^{15}N chemical shift of the amide peak is listed. In the V51 strip, the boxed peak required a 50% deeper level for the peak to be observed. Arrows between peaks illustrate $\alpha N(i,i+1)$ or $NN(i,i+1)$ connectivities in helix 1.

(Bhatnagar *et al.*, 1991), and in all cases at least 85% of the activity remained after prolonged NMR experiments. All other reagents for the enzymatic assay and for the NMR samples were of the highest purity commercially available.

NMR Spectroscopy. NMR spectra of MutT were acquired on a modified Bruker AM 600 NMR spectrometer (Kay *et al.*, 1990; Weber *et al.*, 1992b; Abeygunawardana *et al.*, 1993b) at 32 °C. Samples contained 1.5 mM MutT, 0.1 mM EDTA, 0.34 mM NaN_3, 5–8 mM d_{11}-Tris-HCl, and enough NaCl (19–21 mM) to give an ionic strength equal to 25 mM. The pH was adjusted to 7.4 in H_2O (10% D_2O) and in 100% D_2O (uncorrected for isotope effects). It was necessary to work at these pH conditions due to the reduced stability of MutT at lower pH or pD values.

Nuclear Overhauser effects (NOEs) were collected in two dimensions with unlabeled MutT in D_2O using TPPI phase cycling (Kumar *et al.*, 1980; Marion & Wüthrich, 1983) and mixing times of 100 and 200 ms. 2D ROESY experiments were carried out as described (Kessler *et al.*, 1987) using a 75-ms spin lock time with a 2.8-kHz RF field.

In three dimensions, NOESY-HMQC data (Marion *et al.*, 1989a; Clore *et al.*, 1991) were collected in H_2O with a mixing time of 200 ms, at 600 MHz and 60.8 MHz for ^{1}H and ^{15}N, respectively, as previously described (Kay *et al.*, 1990; Weber *et al.*, 1992b; Abeygunawardana *et al.*, 1993b). To resolve overlapping NH to NH cross peaks in the NOESY-HMQC spectra, HMQC-NOESY-HMQC spectra were acquired with a 200-ms mixing time, as previously described (Ikura *et al.*, 1990).

The NOESY-HMQC and HMQC-NOESY-HMQC data were collected in the phase sensitive mode using the TPPI-States method (Marion *et al.*, 1989b). For the NOESY-HMQC spectra, 64 (complex) points in t_1, 32 (complex) points in t_2, and 1024 (real) points in t_3 were collected in 16 scans per (t_1, t_2) point in a total time of 64 h. The acquisition times were 9.1 ms (^{1}H, t_1), 17.5 ms (^{15}N, t_2) and 63.5 ms (^{1}H, t_3), respectively. The final, three-dimensional data matrix consisted of 256 × 128 × 512 real points in f_1, f_2, and f_3, respectively.

The HMQC-NOESY-HMQC data were collected as described for the NOESY-HMQC data, except that 32 scans per t_1, t_2 point were taken, resulting in a total time of 100 h. The acquisition times were 35 ms (^{15}N, t_1), 17.5 ms (^{15}N, t_2) and 63.5 ms (^{1}H, t_3), respectively. The final three-dimensional data matrix consisted of 128 × 128 × 1024 real points in f_1, f_2, and f_3, respectively. Data were processed on a Personal IRIS (Silicon Graphics Inc.) using the software FELIX (Hare Research Inc., Woodinville, WA) as previously described (Weber *et al.*, 1992b, Abeygunawardana *et al.*, 1993b).

Hydrogen exchange of the amide protons was observed by lyophilizing MutT from H_2O and redissolving it in D_2O. Immediately after the addition of D_2O a series of 2D ^{1}H–^{15}N HSQC spectra were initiated at 0.18, 0.50, 1.0, 1.5, 2.0, 3.0, 10.0, and 24.0 h as described previously (Marion *et al.*, 1989b). In the ^{15}N dimension 512 points were collected using TPPI, and the other experimental parameters are as described (Abeygunawardana *et al.*, 1993b). With two scans, the total experimental time required was 17 min.

Chemical shifts of protons and ^{13}C are reported with respect to external TSP using the HDO resonance of water as a secondary standard (δ = 4.706 ppm from TSP at 32 °C). ^{15}N chemical shifts are with respect to liquid NH_3 using external 2.9 mM $^{15}NH_4Cl$ in 1 M HCl as a secondary standard (δ = 24.93 ppm from liquid NH_3).

Circular Dichroism Spectroscopy. Circular dichroism spectra were recorded as previously described (Chuang *et al.*, 1992) at 23 °C in a nitrogen atmosphere on a AVIV 60 DS spectropolarimeter using quartz cuvettes with a 0.1-mm path length. Samples contained 53 μM MutT 10 mM Tris-HCl buffer, pH 7.4, and 17 mM NaCl. Spectra were the average of five scans made at 1.0 nM intervals, with a 5-s integration time and 1.2 nM bandwidth, and were corrected to the appropriate baseline level with scans of a solution containing the buffer and salt alone. The secondary structures were estimated utilizing the basis sets of Chang *et al.* (1978) and of Perczel *et al.* (1992).

RESULTS

General Approach to Secondary Structure Determination. Short- and medium-range NOE correlations in the 3D NOESY-HMQC spectrum (Figure 1) and in the HMQC-

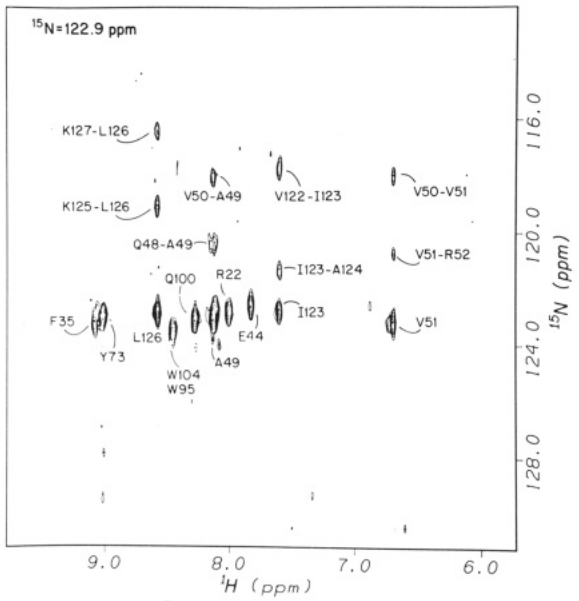

FIGURE 2: Selected ^{15}N plane of the 3D HMQC-NOESY-HMQC spectrum of MutT illustrating regions of both helices. Mixing time is 200 ms. Other conditions are as given in the legend to Figure 1 and under Materials and Methods.

NOESY-HMQC spectrum (Figure 2) of uniformly ^{15}N-labeled MutT were assigned using the HN, ^{15}N, and Hα assignments determined in the preceding paper (Abeygunawardana *et al.*, 1993b) and categorized as strong, medium, or weak (Figure 3). Helical regions of MutT are identified by sequences of residues containing strong NN (i+1), and weaker αN(i,i+1), NN(i,i+2), αN(i,i+3), and αN(i,i+4) NOE cross peaks as described previously (Wüthrich, 1986). Additional pieces of evidence for helical segments are provided by slow amide hydrogen exchange (Wüthrich, 1986), a series of downfield-shifted Hα resonances (Wishart *et al.*, 1992), and a series of upfield shifted Cα resonances (Spera & Bax, 1991) (Figure 3).

β-Strands were identified on the basis of their characteristically strong αN(i,i+1) NOE correlations, sequences of upfield-shifted resonances for the Hα protons (Wishart *et al.*, 1992), and sequences of downfield-shifted Cα resonances (Spera & Bax, 1991). Long-range NOE peaks observed in 2D NOESY spectra of unlabeled MutT in D_2O at mixing times of 100 and 200 ms (Figure 4) and heteronuclear 3D NOESY-HMQC (Figure 1) and HMQC-NOESY-HMQC spectra of ^{15}N-labeled MutT in H_2O (Figure 2) were used in combination with hydrogen exchange data and chemical shift

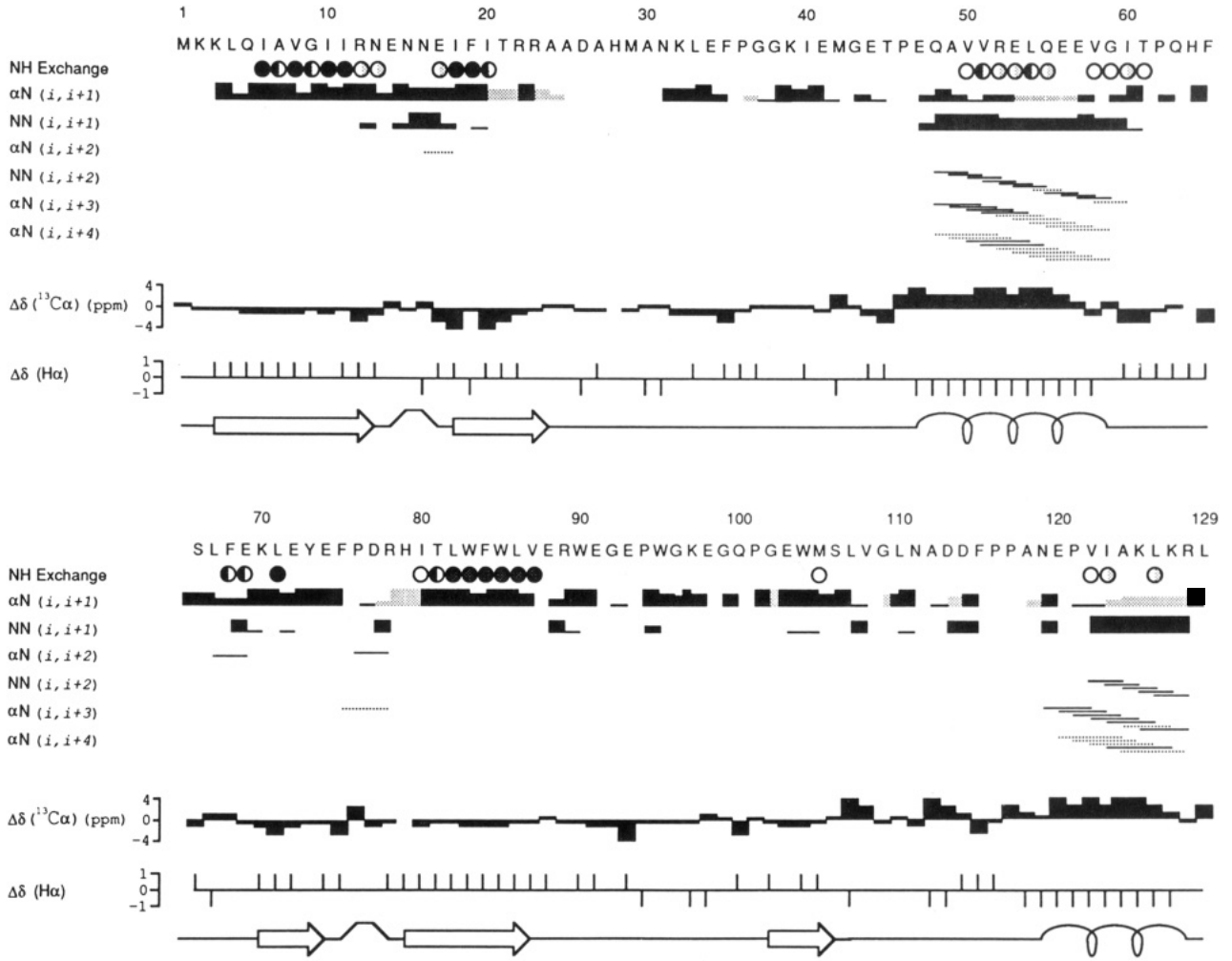

FIGURE 3: Diagram of amide exchange, NOE connectivities, and changes in chemical shifts for MutT. Circles indicate slow amide hydrogen exchange at 32 °C as determined using 2D ^{1}H–^{15}N HSQC spectra as described under Materials and Methods. (Open circles) 11 min < T < 0.5 h; (lightly half-shaded circles) 0.5 h < T < 3 h; (darkly half-shaded circles) 3 h < T < 12 h; and (filled circles) T > 24 h. The NOEs were determined from 3D NOESY-HMQC and HMQC-NOESY-HMQC spectra acquired at 32 °C as described under Materials and Methods. The height of the bar indicates the strength of the NOE peak (strong, medium, weak), and a dashed bar indicates that the NOE is tentatively assigned due to overlaps in chemical shift. $\Delta\delta$ for Hα and Cα resonances are illustrated utilizing the systems of Wishart *et al.* (1992) and Spera & Bax (1991). α-helices (spirals), β-strands (arrows), and turns (bends between arrows) are indicated under the appropriate residues in the sequence.

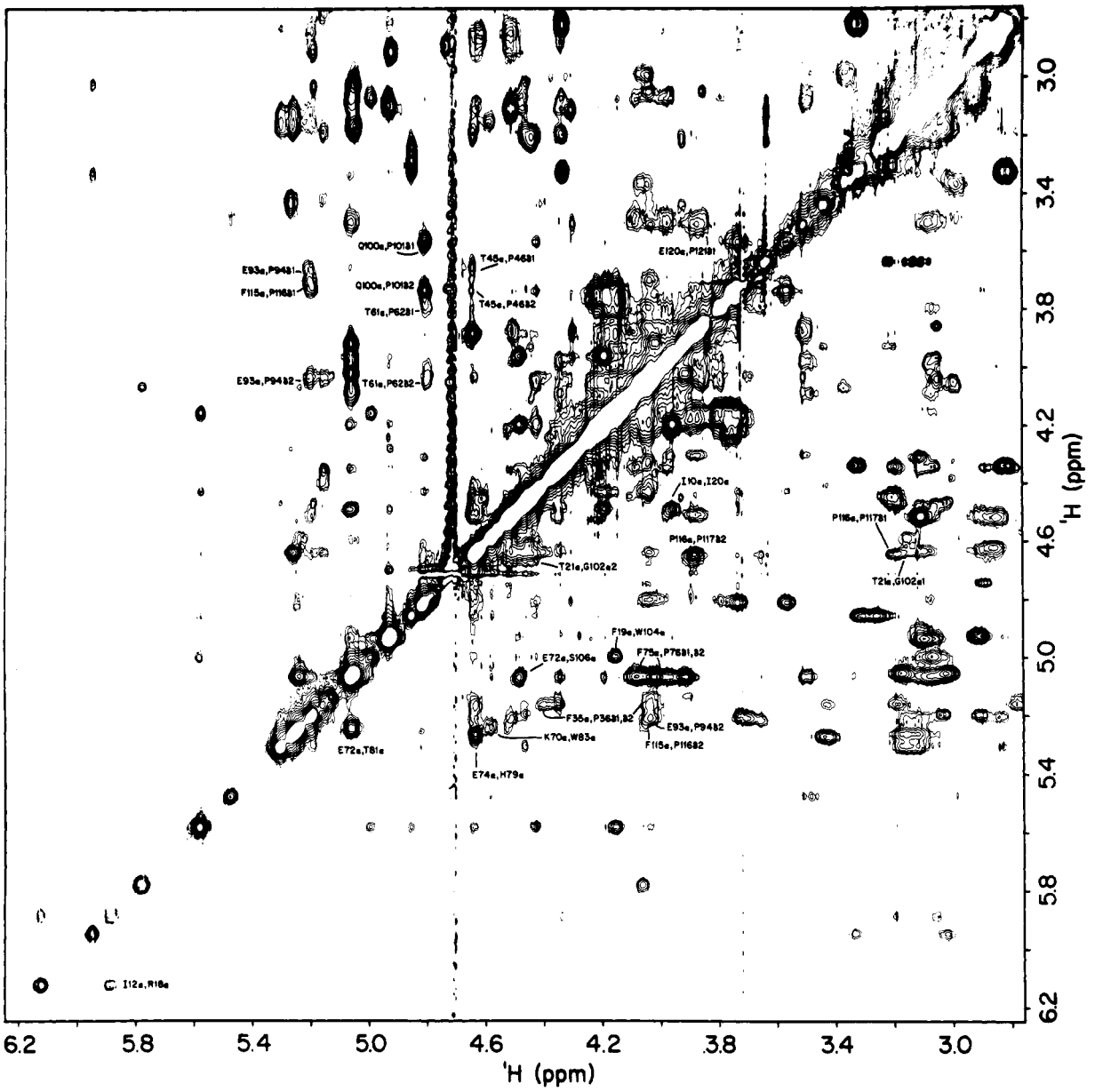

FIGURE 4: Portion of 2D NOESY spectrum in D_2O which displays NOE peaks to Hα protons. Data were collected at 32 °C with a 250-ms mixing time as described under Materials and Methods.

data to define the β-sheet structure (Figure 5). Various tight turns can be delineated by characteristic combinations of αN(i,i+3), αN(i,i+2), αN(i,i+1), NN(i,i+2), and NN(i,i+1) NOEs observed in the 3D NOESY-HMQC and HMQC-NOESY-HMQC as described previously (Wüthrich, 1986). The secondary structural components of MutT derived from these data are described in detail below.[2]

α-Helices. Two helical segments in MutT from residues 47–59 (helix 1) and residues 119–128 (helix 2) contain the characteristic stretches of strong or medium NN(i,i+1) and weaker αN(i,i+1) NOEs (Figures 1 and 2). Furthermore, helix 1 unambiguously shows nine NN(i,i+2), four αN(i,i+3), and two αN(i,i+4) NOE cross peaks, while helix 2 contains five, six, and one of the same NOE connectivities, respectively (Figure 3). Chemical shift overlap of sequential NH, ^{15}N, and αH protons for the other possible NOEs in the helices preclude their unambiguous identification (Figure 3). The method of Wishart *et al.* (1992) assigns the value of +1, 0, or −1 to a residue on the basis of whether the Hα proton is downfield of, within, or upfield of a chemical shift range for a specific amino acid in a random coil. A sequence containing a series of −1 values predicts the presence of an α-helix while a series of +1 values predicts the presence of β-strand. In MutT, helix 1 contains a series of 12 upfield-shifted Hα resonances in sequence from E47 to V58, while helix 2 contains 10 upfield-shifted Hα resonances in sequence from A118 to K127 indicative of helix formation. Furthermore, the deviation from random-coil chemical shifts for the Cα resonances is also utilized for secondary structure prediction. Thus, for Cα resonances in several proteins the secondary shifts are 3.09 ± 1.00 ppm downfield shifted for residues in a helices and −1.48 ± 1.23 upfield shifted for residues in a β-sheet (Spera & Bax, 1991). In MutT two stretches of downfield secondary shifts greater than 2.09 ppm were observed from residues P46 to E56 and from residues E120 to L126 in helices 1 and 2, respectively. Helix 1 and helix 2 contain ten and three slowly exchanging amide protons, respectively (Figure 3), indicative

[2] Assignments utilized here for the side chain protons of the proline residues based on HCCH-TOCSY experiments will be reported in a future publication with all the side chain assignments.

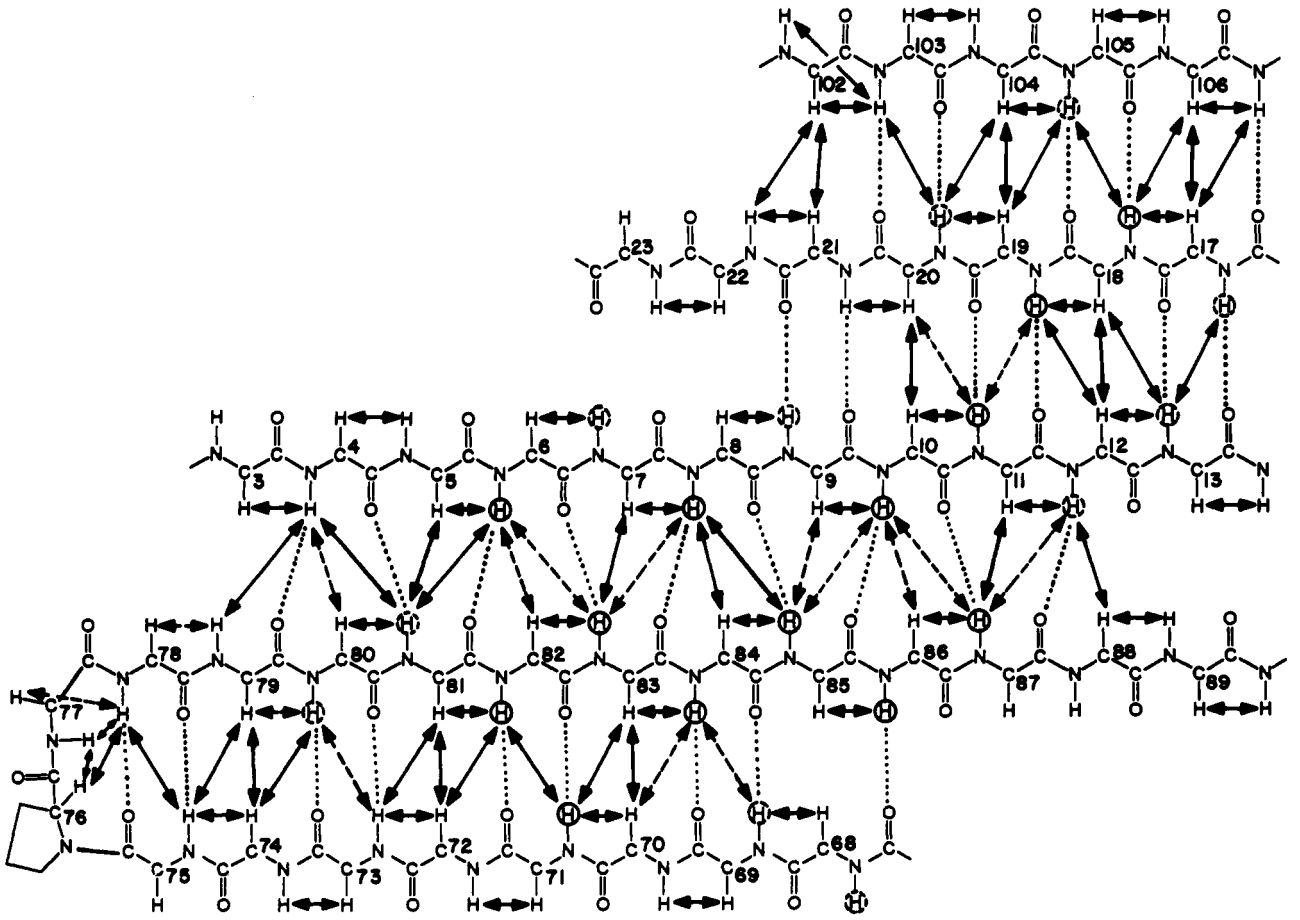

FIGURE 5: Diagram of the β-sheet structure of the MutT enzyme. Long-range HN_i–HN_j, HN_i–$H\alpha_j$, and $H\alpha_i$–$H\alpha_j$ peaks observed (solid lines) in 3D NOESY-HMQC and 2D NOESY spectra. Dashed lines represent NOE peaks that were tentatively assigned due to chemical shift overlap. Dotted lines represent hydrogen bonds derived from slow amide hydrogen exchange (circled protons) and long-range NOEs observed.

Table I: Secondary Structure of MutT As Determined by NMR and CD Spectroscopy

data set CD	α-helix	β-structure	random	average % deviation[a]
Chang *et al.* (1978)[b]	17.5	49.6	32.9	15.4
Perczel *et al.* (1992)[c]	24.2	48.1	27.7	8.2
NMR data[d]	17.8	45.0	37.2	

[a] Average percent deviations were calculated by comparing theoretical curves based on the prediction methods from different basis sets to the circular dichroism data collected for the MutT enzyme. [b] Basis set of Chang *et al.* (1978) containing 15 proteins. [c] Basis set included MutT and 25 other proteins as described by Perczel and Fasman (1992). [d] Estimates for the β-structure includes the β-strands A–E and stretches of MutT sequence predicted to be β-strand by chemical shifts of the Hα and Cα resonances as described previously (Wishart *et al.*, 1992; Spera & Bax, 1991).

of hydrogen bonds expected for a helix. In both cases α-helices rather than 3_{10} helices are indicated by the presence of αN-(i,i+4) connectivities (Wüthrich, 1986). Finally, the percentage of helical residues, 17.8 ± 1.0%, from helixes 1 and 2 determined by NMR agrees with that determined by CD spectroscopy, 20.9 ± 5.4% (Table I).

β-Sheet. Five β-strands (A, 3–13; B, 18–24; C, 70–74; D, 79–87; and E, 102–106) are identified on the basis of the characteristically strong αN(i,i+1) NOEs, a series of uninterrupted downfield-shifted Hα proton resonances, and a series of upfield-shifted Cα resonances (Figure 3) (Wüthrich, 1986; Spera & Bax, 1991; Wishart *et al.*, 1992). Slow amide hydrogen exchange detected in all five strands (Figure 3) indicates that these strands are involved in a hydrogen-bonded multistrand β-sheet structure (Figure 5). This was confirmed by the presence of 34 well-resolved cross-strand NOEs observed in the 2D NOESY spectra in D_2O at mixing times of 100 and 200 ms (Figure 4), arguing against significant spin diffusion artifacts, and in the 3D NOESY-HMQC and HMQC-NOESY-HMQC spectra in H_2O (Figures 1 and 2). Protons in strand A (residues 3–13) were found to give four long-range HN_i–HN_j and five HN_i–$H\alpha_j$ NOEs to protons in strand D (residues 79–87), consistent with the two β-strands aligned in a parallel fashion. Although two long-range HN_i–HN_j NOEs and one HN_i–$H\alpha_j$ NOE peak could tentatively be assigned from each of the residues 4, 6, 8, 10, and 12 on strand A to each of the residues 78, 80, 82, 84, and 86 on strand D, typical for two parallel strands in a β-sheet, only nine of the possible 18 NOEs could be unambiguously assigned due to overlaps in chemical shifts. The presence of nine hydrogen bonds in the two parallel strands is consistent with these long-range NOEs and the eight slowly exchanging amide proton resonances observed between strands A and D. Protons from strand A (residues 10–13) also showed five long-range NOEs to protons of strand B (residues 17–20), including two strong $H\alpha_i$–$H\alpha_j$ NOEs (Figure 4). These long-range NOEs and five slowly exchanging amide NH protons between strands A and B are consistent with an antiparallel alignment with six hydrogen bonds between the two strands as shown in Figure 5. Similarly, strand C (residues 70–74) aligns with strand D (residues 79–87) in an antiparallel fashion to give 10 assignable interstrand NOEs and six slowly exchanging amide NH protons. Strand B (residues 18–24) aligns with strand E

(residues 102–106) in an antiparallel fashion to yield 10 assignable interstrand NOEs and three slowly exchanging amide proton resonances. These alignments predict nine hydrogen bonds between strands C and D and five hydrogen bonds between strands B and E, respectively. The other five interstrand NOEs predicted by the antiparallel β-strands displayed in Figure 5 can only be tentatively assigned due to chemical shift degeneracy and/or weak NOE peaks. Thus, the five-stranded mixed parallel and antiparallel β-sheet structure shown (Figure 5) is based on 34 assigned NOEs, 14 tentatively assigned NOEs, and 22 slowly exchanging NH protons.

Tight Turns. A classical type I tight turn from residues 75 to 78 was indicated by the presence of NN(i,i+1), αN(i,i+2), and αN(i,i+3) NOEs. The NN(i,i+2) NOE is not possible due to a proline being at position 2 in the turn. Furthermore, it has been previously documented that position 2 of a tight turn is the preferred position for a proline as judged by comparing a large number of tight turns in solved protein structures (Richardson, 1981). It was judged to be a type I rather than a type II turn due to its relatively weak αN NOEs throughout the turn (Wüthrich, 1986). No other classical tight turns were found in MutT. However, a nonclassical turn occurs between residues 13 and 17 on the basis of four NN connectivities and of the alignment of the β-sheet. In these five residues the strand reverses direction in order for strand A to run antiparallel to strand B. Consecutive NN connectivities suggesting changes in direction also occur within loops at positions 68–70, 88–90, and 113–115 (Figure 3).

Flexible Regions and Loops. Four loops (I, 24–46); II, 59–70; III, 88–101; and IV, 107–118) adopt an irregular but well-defined structure with the exception of residues in the positions 1–2, 27–28, 43, 112, 118. The latter residues are proposed to be in flexible portions of the protein due to very weak or absent ^1H–^{15}N correlations and lack of intraresidue NOEs. In loop II, which connects helix I to strand C, a series of downfield-shifted Hα chemical shifts and upfield-shifted Cα chemical shifts from positions 60–65 are observed that are suggestive of a β-strand. However, since no long-range NOEs were observed from these residues to strands of the β-sheet network, and since no slowly exchanging amide NH protons were observed in this strand, it was not included in the β-sheet. Similarly, residues 32–37 in loop I and residues 114–116 in loop II show β-strand type Cα and Hα chemical shifts but were not included in the β-sheet due to a lack of interstrand NOE connectivities or slowly exchanging NH protons. Loop I connects strand B to helix 1 and loop IV connects strand E to helix 2. Loop III crosses over strands A and B to connect strands D and E (Figure 6).

Proline Conformations. NOE peaks between proline and its preceding residue, X, can be utilized to distinguish between *cis* and *trans*-X-Pro peptide bonds (Figure 4) based on four criteria (Wüthrich, 1986), which may be expressed in terms of the more common *trans* conformation as two positive and two negative criteria.[2] *Trans* X-Pro shows strong NOEs from the two δ protons of Pro to the Hα of the preceding residue (Hδ^2–Hα$_{i-1}$) and to the NH of the preceding residue (Hδ^2–NH$_{i-1}$), and lacks Hα–Hα$_{i-1}$ and Hα–NH$_{i-1}$ NOEs which are characteristic of *cis* X-Pro. Of the nine prolines of MutT, Pro-94 and 101 are *trans* on the basis of all four criteria, Pro-46, 62, 76, and 121 are *trans* on the basis of three of the four criteria, since overlapping signals prevent application of one of the two negative criteria. Thus Pro-46 and 62 show overlapping signals in the Hα–NH$_{i-1}$ region, and Pro-76 and 121 show overlapping signals in the Hα–Hα$_{i-1}$ region. Pro-36 and -116 are *trans* on the basis of the two positive criteria only since neither of the two negative criteria could be applied due to overlapping signals. Finally, Pro-117 which immediately follows Pro-116, is *trans* solely on the basis of the positive criterion of an Hδ^2–Hα$_{i-1}$ NOE since two other criteria require an NH in the preceding residue and the Hα–Hα$_{i-1}$ region was obscured by overlapping signals. Thus all of the Pro residues of MutT appear to be *trans*. Moreover, no exchange cross peaks were seen in a ROESY experiment in D_2O, and no duplication of spectra was detected, arguing against *cis–trans* isomerization of prolines and multiple enzyme conformations.

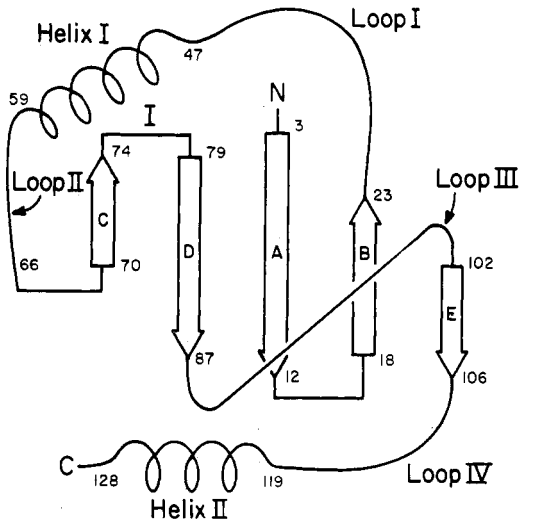

FIGURE 6: Diagram of the secondary structure of MutT.

DISCUSSION

The complete sequence-specific backbone assignments of the protons, carbon, and nitrogen resonances of the MutT enzyme (Abeygunawardana *et al.*, 1993b) have permitted the assignment of more than 600 of the cross peaks in the 2D NOESY and 3D NOESY-HMQC spectra. The evaluation of medium- and long-range NOEs from these data gives rise to a secondary structure for the MutT enzyme consisting of two α-helices and a mixed β-sheet containing five β-strands (A–E) (Figure 6). The β-strands consist of residues A, 3–12; B, 18–23; C, 70–74; D, 79–87; and E, 102–106 (Figures 5 and 6). The β-sheet contains two parallel (p) strands (D and A) within the β-sheet with antiparallel (a) strands on either side such that the β-sheet may be described as C(a)D(p)A(a)B(a)E.

Like MutT, ubiquitin, a smaller protein with 76 residues, contains two helices and a five-stranded mixed β-sheet. However, unlike MutT, in ubiquitin the second helix is a short 3_{10} helix rather than an α-helix, and the alignment of β-strands is B(a)A(p)E(a)C(a)D (Vijay-Kumar *et al.*, 1987; Di Stefano & Wand, 1987; Weber *et al.*, 1987). Several other proteins from the miscellaneous α/β and antiparallel β domain families contain mixed β-sheets consisting of two parallel strands flanked on either side by antiparallel strands. These include protein G (Gronenborn *et al.*, 1991), protein L (Wikström *et al.*, 1993), plakalbumin (Wright *et al.*, 1990), concanavalin A (Reeke *et al.*, 1975), and carbonic anhydrase (Lindskog *et al.*, 1971). While concanavalin A and carbonic anhydrase both have β-strands oriented in a β(a)β(p)β(a)β arrangement, this topology is present in only four strands of 13- and 10-stranded β-sheets, respectively, which in both proteins fold into very elaborate β-sheet networks. On the other hand, in

protein G, protein L, and plakalbumin, the β(a)β(p)β(a)β sheet topology exists solely as a four-stranded sheet.

Small proteins which contain mixed β-sheets show unusually high stabilities. Thus ubiquitin, in which the β-sheet comprises 42% of the residues (Vijay-Kumar *et al.*, 1987; Weber *et al.*, 1987), has a melting temperature (T_m) exceeding 80 °C at pH 5.4 (Lenkinski *et al.*, 1977) and a T_m of 65 °C at pH 2.5.[3] In protein G (56 amino acids) and protein L (61 amino acids), where the β-sheet comprises >50% of the residues, the corresponding melting temperatures (T_m) were found to be 79.4 and 76.5 °C, respectively, at pH 6.0 (Alexander *et al.*, 1992; Wikström *et al.*, 1993). The relatively high stability of these proteins is attributed to a large number of hydrogen bonds in the β-sheet structure (21 hydrogen bonds in ubiquitin, 18 hydrogen bonds in protein L, and 16 hydrogen bonds in protein G) as well as additional hydrophobic interactions. Interestingly, MutT contains 28 hydrogen bonds in its β-sheet network and 22 of the 37 residues in the β-sheet (Figure 2) are hydrophobic, with a particularly high concentration (13 residues) on strands A and D, consistent with these two parallel strands being at the center of a hydrophobic core. The temperature of inactivation for MutT ($T_{inac} \sim 65$ °C at pH 7.5) (Bullions, 1993), which is high for an enzyme, may be lower than the T_m for proteins G and L due to an unusual crossover loop (loop III; residues 88–101) which extends from the end of β-strand D over β-strands A and B to the beginning of β-strand E (Figure 6). In protein G and protein L a similar crossover exists. However, rather than a loop as found in MutT, a helix was found to extend over the two intervening strands to give additional hydrophobic interactions (Wikström *et al.*, 1993; Gronenborn *et al.*, 1991). In ubiquitin, two such crossovers also contain helices (Vijay-Kumar *et al.*, 1987). In a more typical fashion, helix I and loop I of MutT together provide the other two-strand crossover from the C-terminus of strand B over β-strands A and D to the N-terminus of strand C (Figure 6).

In a preliminary search for the active site (Weber *et al.*, 1993b), HSQC titrations of MutT with the essential divalent cation activator Mg^{2+} reveal changes in chemical shifts of HN (≥0.05 ppm) and ^{15}N (≥0.1 ppm) resonances of residues in loops I and III, at the end of helix I, and in β-strands A and B. Subsequent titration with the substrate analog and linear competitive inhibitor Mg^{2+}-AMPCPP reveal chemical shift changes in the same regions but most notably in residues A27, M29, A30, N31, K39, and I40 of loop I. Titration with Mn^{2+}-AMPCPP, a distance-dependent probe, results in the selective disappearance due to paramagnetic broadening of the HN and ^{15}N cross peaks of residues G37, G38 and K39 of loop I, and G57, indicating proximity of the bound substrate analog to loop I and to the end of helix I.

In accord with these findings, a comparison of the amino acid sequence of MutT with those of the same enzyme from *Streptococcus pneumoniae* (MutX) (Bullions *et al.*, 1993) and from *Proteus vulgaris* (MutP) (Bullions, 1993) reveals homologies in loop I from residues 37 to 46 and in the C-terminus of helix I from positions 52 to 59. Mutations in loop I of MutT resulting in the change of Glu-34 to Lys or of Gly-38 to Asp result in the appearance of the mutator phenotype, and the stable, purified E34K enzyme has been shown to have lost at least two orders of magnitude of GTPase activity when compared with the wild-type enzyme, suggesting that residues in loop I are critical to the enzymatic activity and function of MutT (Bullions, 1993).

[3] P. S. Khorasanizadeh and H. Roder, private communication, 1993.

The NMR data and secondary structure presented here provide the basis for elucidating the complete three-dimensional structure of the unliganded and liganded MutT enzyme and the means for designing future mutagenesis studies. Together, these structure/function studies may clarify how loop I and other residues in MutT function in catalyzing the unusual hydrolysis of NTP by nucleophilic substitution at the rarely attacked β-phosphorus.

ACKNOWLEDGMENT

We are grateful to the late Ron Garrett for providing the high quality artwork shown in the figures of this paper and those in many other papers over the years, to Woei-Jer Chuang for analysis of the CD data, and to Peggy Ford for secretarial assistance.

REFERENCES

Abeygunawardana, C., Weber, D. J., Frick, D. N., Bessman, M. J., & Mildvan, A. S. (1993a) *Abstracts of the ENC Conference*, St. Louis, MO, March 14–18 1993, Poster 43, p 94.

Abeygunawardana, C., Weber, D. J., Frick, D. N., Bessman, M. J., & Mildvan, A. S. (1993b) *Biochemistry* (preceding paper in this issue).

Alexander, P., Fahnestock, S., Lee, T., Orban, J., & Bryan, P. (1992) *Biochemistry 31*, 3597–3603.

Bhatnagar, S. K., Bullions, L. C., & Bessman, M. J. (1991) *J. Biol. Chem. 266*, 9050–9054.

Bullions, L. C. (1993) Ph.D. Dissertation, pp 45–70 and 111–112, The Johns Hopkins University, Baltimore, MD.

Bullions, L. C., Maejean, V., Clarerys, J. P., & Bessman, M. J. (1993) *FASEB J.*, A1290.

Chang, C. T., Wu, C.-S. C., & Yang, J. T. (1978) *Anal. Biochem. 91*, 13–31.

Chuang, W-J., Abeygunawardana, C., Pedersen, P. L., & Mildvan, A. S. (1992) *Biochemistry 31*, 7915–7921.

Clore, G. M., & Gronenborn, A. M. (1991) *Prog. Nucl. Magn. Reson. Spectrosc. 23*, 43–92.

Cox, E. C. (1973) *Genetics 73 (Suppl.)*, 62–80.

Di Stefano, D. L., & Wand, A. J. (1987) *Biochemistry 26*, 7272–7281.

Gronenborn, A. M., Filpula, D. R., Essig, N. Z., Achari, A., Whitlow, M., Wingfield, P. T., & Clore, G. M. (1991) *Science 253*, 657–661.

Ikura, M., Bax, A., Clore, G. M., & Gronenborn, A. M. (1990) *J. Am. Chem. Soc. 112*, 9020–9022.

Kay, L. E., Ikura, M., Tschudin, R., & Bax, A. (1990) *J. Magn. Reson. 89*, 496–514.

Kessler, H., Griesinger, C., Kerssebaum, R., Wagner, K., & Ernst, R. R. (1987) *J. Am. Chem. Soc. 109*, 607–609.

Kumar, A., Wagner, G., Ernst, R. R., & Wüthrich, K. (1980) *Biochem. Biophys. Res. Commun. 96*, 1156–1163.

Lenkinski, R. E., Chen, D. M., Glickson, J. D., & Goldstein, G. (1977) *Biochim. Biophys. Acta 494*, 126–130.

Lindskog, S., Henderson, L. E., Kannan, K. K., Liljas, A., Nyman, P. O., & Strandberg, B. (1971) in *The Enzymes* (Boyer, P. D., Ed.) Vol. 5, pp 608–622, Academic Press, New York.

Marion, D., & Wüthrich, K. (1983) *Biochem. Biophys. Res. Commun. 113*, 967–974.

Marion, D., Driscoll, P. C., Kay, L. E., Wingfield, P. T., Bax, A., Gronenborn, A. M., & Clore, G. M. (1989a) *Biochemistry 28*, 6150–6156.

Marion, D., Ikura, M., Tschudin, R., & Bax, A. (1989b) *J. Magn. Reson. 85*, 393–399.

Mo, J.-Y., Maki, H., & Sekiguchi, M. (1992) *Proc. Natl. Acad. Sci. U.S.A. 89*, 11021–11025.

Perczel, A., Park, K., & Fasman, G. D. (1992) *Anal. Biochem. 203*, 83–93.

Reeke, G. N., Becker, J. W., & Edelman, G. M. (1975) *J. Biol. Chem. 250*, 1525–1547.

Richardson, J. (1981) *Adv. Protein Chem. 34*, 167–339.

Rost, B., Schnéider, R., & Sander, C. (1993) *Trends Biochem. Sci. 18*, 120–123.

Spera, S., & Bax, A. (1991) *J. Am. Chem. Soc. 113*, 5490–5492.

Treffers, H. P., Spinelli, V., & Belser, N. O. (1954) *Proc. Natl. Acad. Sci. U.S.A. 40*, 1064–1071.

Vijay-Kumar, S., Bugg, C. E., & Cook, W. J. (1987) *J. Mol. Biol. 194*, 531–544.

Weber, D. J., Abeygunawardana, C., Frick, D. N., Bessman, M. J., & Mildvan, A. S. (1993a) *FASEB J.*, A1289.

Weber, D. J., Bhatnagar, S. K., Bullions, L. C., Bessman, M. J., & Mildvan, A. S. (1992a) *J. Biol. Chem. 267*, 16939–16942.

Weber, D. J., Gittis, A. G., Mullen, G. P., Abeygunawardana, C., Lattman, E. E., & Mildvan, A. S. (1992b) *Proteins: Struct., Funct., Genet. 13*, 275–287.

Weber, D. J., Abeygunawardana, C., Frick, D. N., Gillespie, J. R., Koder, R. L., Bessman, M. J., & Mildvan, A. S. (1993b) *Abstr. Eastern Anal. Symp.*, Nov. 15–19, 1993, Somerset, NJ.

Weber, P. L., Brown, S. C., & Mueller, L. (1987) *Biochemistry 26*, 7282–7290.

Wikström, M., Sjöbring, U., Kastern, W., Björck, L., Drakenberg, T., & Forsèn, S. (1993) *Biochemistry 32*, 3381–3386.

Wishart, D. S., Sykes, B. D., & Richards, F. M. (1992) *Biochemistry 31*, 1647–1651.

Wright, H. T., Qian, H. X., & Huber, R. (1990) *J. Mol. Biol. 213*, 513–528.

Wüthrich, K. (1986) *NMR of Proteins and Nucleic Acids*, John Wiley, New York.

Yanofsky, C., Cox, E. C., & Horn, V. (1966) *Proc. Natl. Acad. Sci. U.S.A. 55*, 274–281.